5th International Symposium on Three-Dimensional Electromagnetics
Sapporo, Japan, May 7–9, 2013

3D electromagnetic modeling using multi-resolution approach

Maria Cherevatova[1], Gary D. Egbert[2], Maxim Yu. Smirnov[1] and Anna Kelbert[2]
[1]University of Oulu, Finland
[2]Oregon State University, Oregon, USA

SUMMARY

We present a multi-resolution approach for 3D forward electromagnetic (EM) modeling and inversion. Development of the technique is motivated by the fact that a finer grid resolution is often required in the near surface to adequately represent near surface inhomogeneities and topography. On the other hand, the EM fields propagate in a diffusive manner and can be sufficiently well described on a grid that becomes gradually coarser with depth. A multi-resolution approach, therefore, provides a means to significantly decrease the number of degrees of freedom and hence improve on computational efficiency without significantly compromising the accuracy of the solution.

In our implementation, the full grid is represented as a vertical stack of sub-grids, each of which is a standard staggered grid. The grid is refined only in the horizontal direction, uniformly across vertical layers, allowing only factor of two between vertically adjacent sub-grids, and is thus a simplified quadtree scheme. In the present work we describe the grid design and setting of the corresponding operators.

A major difficulty lies in discretizing the forward operator around the interfaces. To maintain efficiency of iterative solvers, and to simplify adjoint sensitivity calculations for inversion applications it is desirable to preserve symmetry of discretized operators. In particular, the discretized operator $\nabla \times \nabla \times$ needs to be self-adjoint, and the operators $\nabla \cdot$ and ∇ should be adjoints of each other (with respect to appropriate inner products). We describe a first order accurate approach to compute these operators that preserves these symmetries. We have run synthetic tests to compare 3D solver accuracy relative to 2D solution. The responses through the center of the infinite prism and corresponding 2D cube model yields phase difference of 0.2 °. The improvement in speed of forward solver reaches 3 – 6 times and memory requirements 1.5 – 3 for the larger models.

Keywords: multi-resolution, forward modeling, inversion, finite difference

INTRODUCTION

We consider an extension of the staggered-grid discretization of (Yee, 1966) to a multi-resolution grid. Our approach is similar to the octree scheme of Haber & Heldmann (2007); Horesh & Haber (2011), where each grid cell can be subdivided in half in each direction. However, we allow grid refinement in only the horizontal directions, using a quadtree scheme (Finkel & Bentley, 1974). We make the further assumption that the grid refinement is constant over a vertical level. This allows us to represent the full grid as a vertical stack of sub-grids, each of which is a standard structured staggered grid, connected at a series of layers interfaces. This allows us to apply operators and functions already developed for a simpler standard structured grid to the interior nodes of each sub-grid. However, operators on the interfaces between adjacent sub-grids must be modified. For convenience we allow only factor of two between adjacent sub-grids.

Note that in the forward EM modeling approaches of Haber & Heldmann (2007) and Horesh & Haber (2011) octree refinement was used as part of multi-grid solver. Here we use the grid refinement to reduce problem size, but still solve the linear system of equations iteratively using a quasi-minimum residuals scheme, with an ILU preconditioner.

The ModEM 3D magnetotelluric (MT) inversion software (Egbert & Kelbert, 2012) is used as a basis for implementation of the multi-resolution forward modeling scheme. With relatively minor additional modifications (primarily to the model parameter mapping) the new forward solver can then be used for 3D inversion. In the staggered grid convention realized in ModEM, the discretized electric field vector components are defined on cell edges. The magnetic fields are therefore defined on cell faces. Thus, the discrete representation of second order PDEs derived from Maxwell's equations can be expressed as a discrete system on the interior nodes as

$$[\mathbf{C}^{\dagger}\mathbf{C} + diag(i\omega\mu\sigma(\mathbf{m}))]\mathbf{e} = 0. \quad (1)$$

Here $diag$ denotes a diagonal matrix, $\mathbf{C}$ is the discrete approximation of the curl operator (mapping interior cell edge vectors to interior cell faces), $\mathbf{C}^{\dagger}$ is the discrete adjoint of the curl (mapping interior cell face vectors to interior cell edges). Finally, $\sigma(\mathbf{m})$ represents the mapping of the model parameters $\mathbf{m}$ (conductivity or resistivity (or its logarithm)) to cell edges, where the electric field components are defined. The discrete curl operator $\mathbf{C}$ and its adjoint must be defined in the interior of the sub-grids and their interfaces.

DISCRETIZATION OF THE ADJOINT OF THE CURL ON THE INTERFACES

The major difficulty in discretizing Maxwell's equations on locally refined meshes lies in discretizing the $\nabla\times\nabla\times$ operator around interfaces between varying cell sizes. The adjoint of the $\nabla\times$ operator ($\mathbf{C}^{\dagger}$) maps faces onto edges. However some interface edges do not have neighbors in the coarser of the two meshes (see Figure 1). For the first order accuracy we compute the adjoint of the curl using 1, 2, 3 and 4 faces or 3, 5, and 6, depending on the nature of the boundary edge. This approach has the advantage of guaranteeing symmetry of the $\mathbf{C}^{\dagger}\mathbf{C}$ operator, simplifying the development of adjoints required for computing sensitivities. In order to obtain second order accuracy (comparable to the original staggered grid) "ghost" edges need to be introduced (Horesh & Haber, 2011). Such an approach is expected to improve forward solver accuracy, but will complicate sensitivity calculations due to the fact that forward operator is no longer symmetric. The loss of symmetry may also warrant alternative iterative solvers and/or preconditioners. We are currently developing this alternative approach to operator discretization, and expect to present initial results at the workshop.

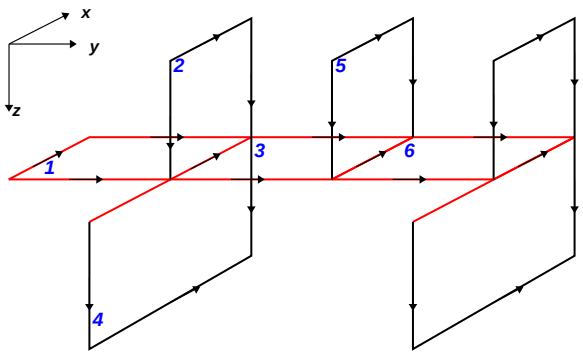

Figure 1. Discretization of the $\mathbf{C}^{\dagger}\mathbf{C}$ operator on the interfaces. Red color represents interface layer from finer to coarser sub-grids.

DISCRETIZATION OF THE DIVERGENCE ON THE INTERFACES

One of the important steps in implementing the forward solver is the so-called divergence correction. In the ModEM finite difference forward solver, the flux density vectors $\mathbf{J} = \sigma\mathbf{e}$ are defined on cell edges. Thus, the discrete gradient operator, which maps from the potential defined on cell nodes to cell edges, has an obvious definition. However, the adjoint of this operator, the divergence, which maps interior cell edge vectors to interior cell nodes (Figure 2) is more complicated, since some nodes on interfaces between coarser and finer sub-grids have no neighbor edges in the coarser sub-grid. Using the approach sketched in Figure 2 again yields a dicrete $\bigtriangledown\cdot\sigma\bigtriangledown$ operator that is symmetric, but only first order accurate (Haber & Heldmann, 2007).

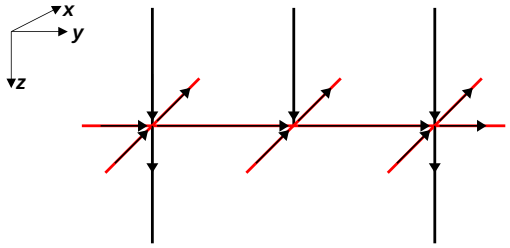

Figure 2. Discretization of the divergence on the interfaces. Red color represents interface layer from finer to coarser sub-grids.

MODEL PARAMETRIZATION

The model parameters are defined for the cell centers, and needs to be computed on multi-resolution grid edges for input to (1). The natural mapping from the cell centers to the edges of a regular grid requires multiplication by the operator $\mathbf{W} = \mathbf{V}_E^{-1}\tilde{\mathbf{W}}\mathbf{V}_C$, where $\mathbf{V}_E$ and $\mathbf{V}_C$ are diagonal operators that multiply by volume elements centered around the grid edges and the cell centers, respectively, and $\tilde{\mathbf{W}}$ is the unweighted averaging operator that sums the values in the four cells bordering every edge, then divides by four. The conductivity mapping is given by $\sigma(\mathbf{m}) = \mathbf{W}\mathbf{m}$ or $\sigma(\mathbf{m}) = \mathbf{W}exp(\mathbf{m})$, for the cases of linear and log conductivity, respectively. We define the conductivity parametrization on the fine grid, so in the multi-resolution case we need to consider additional averaging from fine to coarse sub-grids. Therefore, apart from the averaging operator $\mathbf{W}$ from cells to cell edges, weighted by volume elements, we define an additional linear mapping $\mathbf{A}$ from the edges of the fine grid, to the edges of the multi-resolution grid. Therefore the conductivity parameter mapping can be expressed as $\sigma(\mathbf{m}) = \mathbf{A}\mathbf{W}\mathbf{m}$. Transpose of the weighted averaging

operator $\mathbf{W}^T = \mathbf{V}_C \tilde{\mathbf{W}}^T \mathbf{V}_E^{-1}$ represents a mapping from cell edges to cells, which is a weighted sum of contributions from all edges that bound a cell. In conjunction with the adjoint of the operator $\mathbf{A}$, which defines the interpolation from the multi-resolution grid edges to the edges of the fine grid, $\mathbf{W}^T \mathbf{A}^T$ represents the adjoint mapping from the edges of multi-resolution grid to the cells of the original (fine) grid where the model parameter is defined. This is used to calculate the sensitivities for gradient-based inversion.

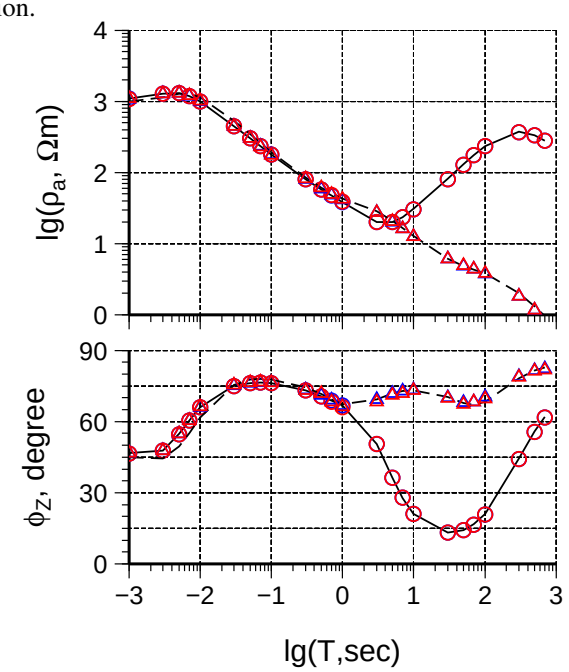

Figure 3. Accuracy of the forward solution. Comparison of the MT sounding curves over the center of the 2D prism. 2D forward responses computed from ModEM 2D: black solid line – Z_{yx}, dashed line – Z_{xy}. 3D responses computed from ModEM 3D original version: blue open circle – Z_{yx}, blue triangle – Z_{xy}. 3D responses computed from ModEM MG 3D with five coarseness levels: red open circle – Z_{yx}, red triangle – Z_{xy}.

EXAMPLES

Numerical accuracy

Since the accuracy of a 2D solver is well known, it can be used as a reference. We thus compare the 2D solution, ModEM MG 3D and standard ModEM 3D solutions. The synthetic model represents an infinite 2D prism of size 10×4.3 km and 10 Ωm resistivity, embedded in a 1000 Ωm half-space at the depth of 1.7 km. The size of the grid was 64x64x52 cells. The quadtree grid consisted of 5 sub-grids, two air sub-grids and three sub-grids inside the Earth. The corresponding 2D model was solved on the 64x52 cells grid. In Figure 3, the MT sounding curves at a site over the center of the conductive prism are shown. The periods range from 10^{-3} to 700 s with 4 periods per decade.

Comparison shows that resistivities fit well for both modes. Phase difference for TE mode is 0.2 ° between 3D original and 2D responses and 0.8 ° between 3D multi-resolution and 2D responses at maximum. For TM mode, phase differs for 3 ° at maximum in both cases (original and multi-resolution). The difference in apparent resistivities is 2% at maximum.

Speed-up

In order to evaluate the performance and speed of our multi-resolution grid solution we tested different grid sizes ($N_x \times N_y$) = 16^2, 32^2, 64^2, 128^2, 256^2, 512^2 and 1024^2 cells, and N_z = 52 layers by z for all models. The largest problem we solve (1024^2) corresponds to 54,525,952 model parameters for the fine uniform grid (original ModEM 3D) and requires 17.1 GB RAM. The multi-resolution grid for this problem has only 5,592,672 cells distributed between 16 sub-grids and requires 7.3 GB RAM to run and takes 9.5 minutes for one forward solution.

Table 1. Speed-up for the test problem with the Cube (512 and 1024 for half-space (HS)). Abbreviations: *or* – original ModEM 3D, *mg* – multi-resolution version ModEM MG 3D; N_{or}/N_{mg} – ratio of the numbers of the model parameters, t_{or}/t_{mg} – ratio of the solution time.

Model type	N_{or}/N_{mg}	t_{or}/t_{mg}
16	1.8	0.7
32	2.4	1.5
64	1.7	1.3
	2.5	1.3
	4.9	1.7
128	1.8	1.5
	2.5	1.4
	4.9	2.4
256	2.5	3.3
	4.9	5.6
512 HS	4.9	4.6
1024 HS	4.9	-

The large forward problems (512 and 1024) were tested for the half-space of 1000 Ωm and showed performance of the multi-resolution grid of 4 to 6 times faster than original ModEM 3D (Table 1). The rest of the models were tested for the conductivity contrast of 10 Ωm vs 1000 Ωm background, the parameters of the model described above. Table 1 demonstrates the dependence of the number of the model parameters from the computational time for forward solution. We see a significant increase of the computational time ratio between original ModEM 3D (t_{or}) and

multi-resolution ModEM MG 3D (t_{mg}) with the number of the model parameters.

CONCLUSIONS

In this work we developed a quadtree approach for the numerical solution of 3D electromagnetic forward problem. We have discussed the discretization of the forward problem on this multi-resolution grid and defined operators on the interfaces. The accuracy of the multi-resolution forward solver is within 2% compared to original 3D solution and allows computations to be speed up by several times; the scheme also has a smaller memory foot print. Therefore, inversion based on the multi-resolution grid forward solver might provide a significant computational advantages, and also allow greater flexibility in terms model discretizations and better resolution of near-surface features. Future work will involve testing alternative solvers for the system of linear equations as we seek to construct more accurate solutions without sacrificing speed.

REFERENCES

Egbert, G. D., & Kelbert, A. (2012). Computational recipes for electromagnetic inverse problems. *Geophysical Journal International*, *189*(1), 251–267.

Finkel, R., & Bentley, J. (1974). Quad trees a data structure for retrieval on composite keys. *Acta Informatica*, *4*, 1-9.

Haber, E., & Heldmann, S. (2007). An octree multigrid method for quasi-static Maxwell's equations with highly discontinuous coefficients. *Journal of Computational Physics*, *223*, 783-796.

Horesh, L., & Haber, E. (2011). A Second Order Discretization of Maxwell's Equations in the Quasi-Static Regime on Octree Grids. *SIAM J. on Scientific Computing*, *33*, 2805-2822.

Yee, K. S. (1966). Numerical Solution of Initial Boundary Value Problems Involving Maxwell's Equations in Isotropic Media. *IEEE. Trans. Anten. Propag.*, *14*(3), 302–307.